İSTANBUL UNIVERSITY PRESS

International Journal of Environment and Geoinformatics
2025, 12 (2): 45–57

https://doi.org/10.26650/ijegeo.1661834

Submitted: 20.03.2025
Revision Requested: 18.05.2025
Last Revision Received: 20.05.2025
Accepted: 20.05.2025

International Journal of Environment and Geoinformatics

Research Article

Open Access

Predicting Winter Wheat Yield using Landsat 8-9 Based Vegetation Indices in Semi-Arid Regions

Neslişah Civelek [1], Levent Genç [2] & Özgün Akçay [3]

[1] Çanakkale Onsekiz Mart University, Department of Geographic Information Technologies, Çanakkale, Türkiye
[2] Çanakkale Onsekiz Mart Üniversitesi, Faculty of Architecture and Design, Department of Urban and Regional Planning, Çanakkale, Türkiye
[3] Çanakkale Onsekiz Mart University, Geomatic Engineering, Çanakkale, Türkiye

Abstract This study investigated the prediction of winter wheat yield in cultivation regions of Kumkale (Batakovası) Plain in Çanakkale Province, Türkiye, utilizing Landsat 8-9 imagery-based Vegetation Indices (VIs) alongside Machine Learning (ML) methodologies. The VIs dataset was created by calculating images collected during the 2022 and 2023 growth seasons. The resulting dataset was employed in a C4.5 Decision Tree (DT) algorithm to predict winter wheat yield. The findings indicated that winter wheat yield could be predicted in April for fields classified as 'Low Yield, 'Medium Yield,' and 'High Yield' utilizing all indices except for Enhanced Vegetation Index (EVI) and Soil Adjusted Vegetation Index (SAVI). Interestingly, High Yield' fields could also be predicted in March using the EVI index and in February using the SAVI index. In the winter wheat yield estimation, NDVI with a performance rate of 97.5% was able to determine "High Yield," "Medium Yield," and "Low Yield" in April (heading-blooming), while the lowest performance was with EVI at 77.50%, determining "High Yield" in April (heading-blooming), "Medium Yield" (tilling-jointing) in February, and "Low Yield". (tilling-jointing) in March. The study concluded that winter wheat yields can be predicted using VIs independently of climate data. Future research will concentrate on assessing yield predictions for additional crops by employing various ML algorithms alongside climate data and VIs derived from higher-resolution satellite imagery.

Keywords Winter wheat yield · Landsat 8-9 · Decision tree · Vegetation indices · Machine learning

Citation: Civelek, N., Genç, L. & Akçay, Ö. (2025). Predicting winter wheat yield using landsat 8-9 based vegetation indices in Semi-Arid regions. *International Journal of Environment and Geoinformatics*, *12*(2), 45-57. https://doi.org/10.26650/ijegeo.1661834

Corresponding author: Levent Genç leventgc@comu.edu.tr

Introduction

Vegetation indices (VIs), which are derived from Remote sensing (RS) data, have become increasingly effective in monitoring land cover land use and dynamics of plant phenology over time, as well as in collecting both physiological and physical characteristics of plants. The VIs derived from RS data into information that enhances our understanding of the distribution, characteristics, and ecological significance of crop production areas and other vegetation within natural environments (Cai et al., 2010; Naqvi et al., 2018; Kobayashi et al., 2020; Zhou et al., 2022; Ayub et al., 2022; Jamali et al., 2023). When RS data transform into VIs through methodologies such as Machine Learning (ML), it can be significantly enhanced agricultural production facilitating prompt and precise decision-making (Naqvi et al., 2018; Campos et al., 2019; Liu et al., 2022). The VIs include the Normalized Difference Vegetation Index (NDVI), Green Normalized Difference Vegetation Index (GNDVI), Enhanced Vegetation Index (EVI), Renormalized Difference Vegetation Index (RDVI), Soil Adjusted Vegetation Index (SAVI), Modified Soil Adjusted Vegetation Index (MSAVI), Modified Chlorophyll Absorption Reflectance Index (MCARI), and Wide Dynamic Range Vegetation Index (WDRVI) were extensively utilized to monitor crop development, and determine the timing and intensity of phenological events (Naqvi et al., 2018;Toscano et al., 2019; Segarra et al., 2020; Zhen et al., 2020; Nagy et al., 2021;Qi et al., 2022; Saad El Imanni et al., 2022;Wang et al., 2022; Jamali et al., 2023; Khan et al., 2023; Skendzic et al., 2023; Deng et al., 2022).

The VIs have been shown to predict winter wheat yields effectively over large areas in many studies and farming practices, especially when combined with climate data. These studies mainly used ML methods like Support Vector Machines (SVM), Artificial Neural Networks (ANN), and Deep Neural Networks (DNN) along with climate data to improve predictions of crop yields. Particularly when paired with climatic data, the VIs have been demonstrated in several research and farming operations to reasonably forecast winter wheat yields across considerable regions. This research mostly used climatic data with ML such as Support Vector Machines (SVM), Artificial Neural Networks (ANN), and Deep Neural Networks (DNN) to enhance forecasts of agricultural yields. While Xi et al. (2019) implemented SVM classification in the Bardhaman area, Ayub et al. (2022) used Random Forest (RF) classification in the Faisalabad region of Punjab among the other techniques used to forecast agricultural productivity. Goldberg et al. (2021) implemented RF, SVM, Extreme Gradient Boosting (XGBoost), and Area Under the Curve (AUC) classification techniques in eastern Mediterranean cost. Furthermore, Liu et al. (2022) employed both RF and Deep Learning (DL) classifications in North Henan Province, China. The study of images from various sources to find out what influences plant growth and crop yield tracked through plant growth analysis using ML on Google Earth Engine (GEE) has greatly enhanced farming outcomes all over the world.

Using the idea of entropy produced from the training dataset, the application of RS based VIs coupled with the C4.5 Decision Tree (C4.5-DT), ML approach, for crop yield prediction for categorization by shows different applications across several disciplines (Navada et al., 2011). Based on the input data, the output functions as a decision-support tool that graphically shows a model in the form of a tree, therefore defining decisions and their possible results for a target variable (Gupta et al., 2017). The C4.5-DT algorithm automatically prunes trees (Mallissery et al., 2013), therefore generating smaller trees, simpler rules, and better interpretable findings (Syamala Devi et al., 2016; Deng et al., 2022). High precision pictures can be difficult even if VIs applied in ML techniques are judged as appropriate for detecting product patterns and calculating yields to grasp spatial-temporal variations (Thieme et al., 2020). Many elements affect the accuracy of yield prediction models: terrain structure, RS techniques, field observations, and crop phenological stages depending on the objectives of research. Literary works abound in evidence that climate directly affects the phenological stages as well as plant biological processes (Zhen et al., 2020; Adeniyi et al., 2020; Qiao et al., 2024). Apart from VIs, Leaf Area Index (LAI) and other growth indicators influenced by environmental circumstances can be directly applied in yield prediction models (Panda et al., 2010). Recently, without considering climate data, research conducted just using VIs to forecast agricultural plant yield indicator, LAI. Based just on RS based VIs without climate data, Qiao et al. (2024) constructed LAI estimating models for winter wheat, corn, and soybeans. These results highlight the need of using solely VIs to forecast agricultural crop yields in order to enable fast and low cost effective models employing ML algorithms to enable sustainable agricultural output.

The main objective of this research is to construct predictive models for winter wheat yield prior to harvest by leveraging a diverse set of Vis (NDVI, GNDVI, EVI, RDVI, SAVI, MSAVI, MCARI, and WDRVI) extracted from Landsat 8-9 imagery. Furthermore, the study seeks to ascertain the optimal temporal framework for yield prediction, correlating the VIs with distinct phenological stages, determined monthly. Notably, climate data has been deliberately omitted from the ML-enabled C4.5 DT model, thereby emphasizing an analysis predicated solely on the RS based VIs. This methodological

framework underscores the potential of RS data to facilitate precise prediction of agricultural yields, while concurrently contributing to the advancement of sustainable agricultural methodologies.

Materials and Methods

Study Area

The selected study area is the Çanakkale/Kumkale-Batak Plain, located on the Anatolian side of the Çanakkale Strait (Fig. 1). This region is situated at the mouth of the Aegean Sea on the Anatolian side of the Çanakkale Strait, approximately 27 km from the provincial center (Inalpulat and Genc, 2019).

Data and pre-processing

Field Data: The study area included 40 parcels planted with winter wheat, selected from November to December 2022. The fields were cultivated under both dry and irrigation conditions and were harvested in June 2023. The yield was calculated for 9 parcels using randomly selected 1 square meter (sqm) areas inside the parcels (Table 1 and Figure 2). During the first 3 weeks of June 2023, we collected field data the day before farmers started harvesting. The number of stems in 1 sqm of plants and the number of grains in each head were counted. In the laboratory, 1000 grains from a 1 sqm area with three replications were randomly selected and weighed. It was discovered that the calculated yields closely matched those reported by the farmers (R^2 = 0,98). Therefore, yield data for the remaining 40 parcels was added to the database, considering the farmers' reports. Generally, farmers reported their winter wheat yield as lower than the actual value due to harvesting losses of 1-2%. Lucilla and Masaccio are the common varieties of bread winter wheat grown in the region.

Yield calculations in kilograms (kg) per decare (da) were based on measured data from the field and samples taken from 9 plots. Three examples are as follows: If the number of heads per sqm is 410, the number of grains per head is 25, an average of 10 heads, and the weight of 1000 grains is 42 grams (g) (with 3 repetitions), then the yield is 472 kg/da (compared to the farmer's statement of 450 kg/da) (Parcel 5). If the number of heads per sqm is 631, the number of grains per head is 36, an average of 10 heads, and the weight of 1000 grains is 56 g (with 3 repetitions), then the yield is 1272,09 kg/da (compared to the farmer's statement of 1250 kg/da). (Parcel 25) If the number of heads per sqm is 590, the number of grains per head is 33, an average of 10 heads, and the weight of 1000 grains is 51g (with 3 repetitions), then the yield is 1031 kg/da (compared to the farmer's statement of 1000 kg/da). Although the annual average rainfall in the study area is 625 mm, irrigation was conducted at least once in 33 plots during the phenology stages, with the application of Diammonium Phosphate (DAP) base fertilizer (25 kg/da) and 25 kg/da of urea fertilizer.

Satellite data: Satellite images from Landsat 8-9 for the winter wheat growing season of 2022-2023 (Figure 3 and Table 2) are used to generate VIs using user-friendly library adjustments within the GEE open data source (Aghlmand et al., 2021). The Landsat images were initially cropped according to the study area boundaries, and temporal filtering was applied based on the study period (Esfandabadi et al., 2021). Available images included the months of December, February, March, April, May,

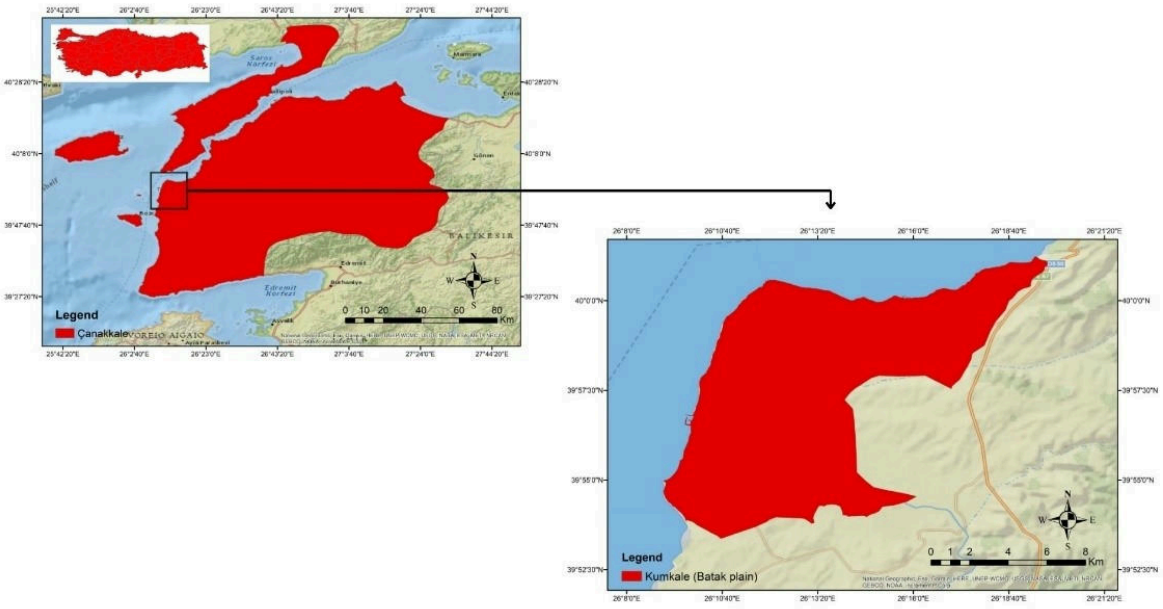

Figure 1. Study area, Batakovası/Çanakkale, Türkiye (Adopted from Inalpulat and Genc, 2019).

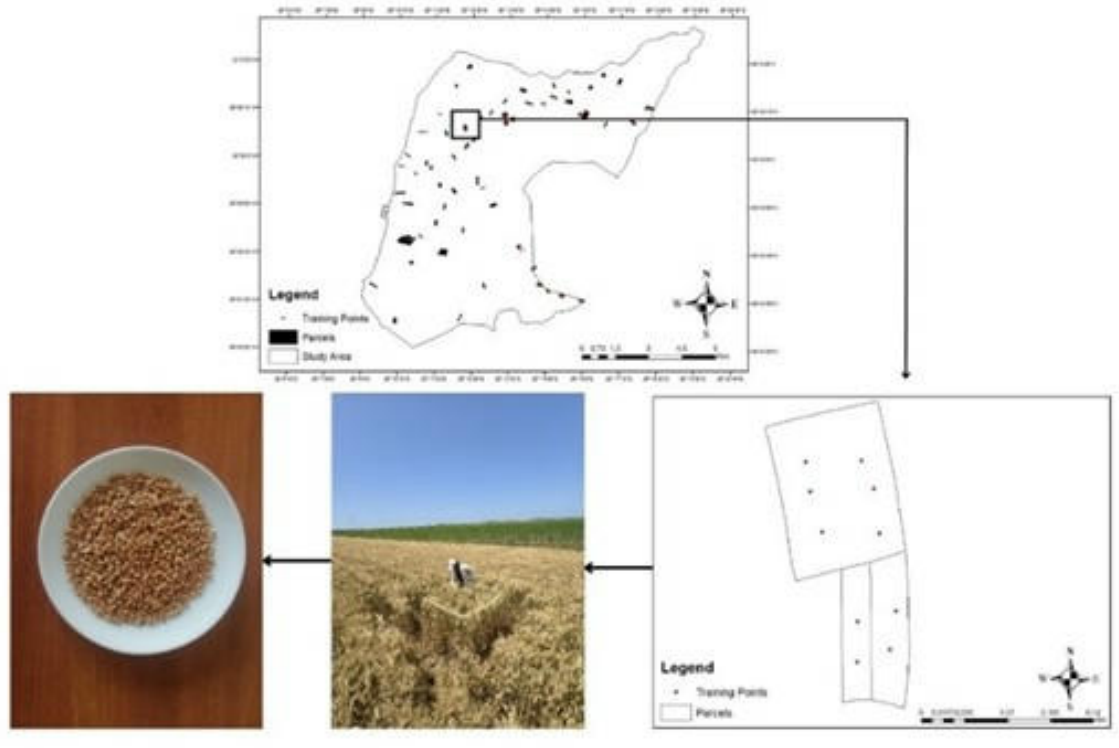

Figure 2. Sampling size and methods.

and June were used to create the new band combination of Landsat images ('B2', 'B3', 'B4', 'B5', 'B6', and 'B7') for the 2022 and 2023 growing seasons (Figure 3, Table 2). Selected VIs was calculated using combined time series images over the study area. The VIs described and formulated in Table 3 are NDVI, which calculates values using red and near-infrared bands, ranges from –1 to 1, and is indicative of changes in the crop growth process (Wang et al., 2022). Similarly, GNDVI employs the green wavelength instead of the red wavelength (Jamali et al., 2023). EVI is primarily used to assess the quality and quantity of vegetation cover (Toscano et al., 2019; Qi et al., 2022; Saad El Imanni et al., 2022), while RDVI, SAVI, and MSAVI have been employed in the analysis of various phenology stages and are often preferred in conjunction with other indices (Segarra et al., 2020; Nagy et al., 2021; Skendzic et al., 2023). Additionally, MCARI is frequently utilized to ascertain chlorophyll density in plants (Zhen et al., 2020; Khan et al., 2023), and WDRVI enhances the correlation among plant canopy characteristics by accurately estimating the relationships within plant canopies (Naqvi et al., 2018) (Table 3).

The VIs values were calculated individually for 40 parcels by averaging between 1 to 6 pixels, contingent upon the size of each parcel. This method ensured that the VIs accurately represented the characteristics of each land parcel. Subsequently, these averaged VIs values were exported to create a comprehensive database, facilitating further analysis and interpretation of the data associated with the winter wheat phenology stages.

During the acquisition of RS data, reflections from objects can occasionally yield extreme values due to various environmental factors (Purwanto et al., 2022). As a result, it may be necessary to correct pixels with values significantly deviating from the meaning to ensure suitability for desired statistical analysis. This process involves applying mathematical generalizations according to Toscano et al., 2019 (Eq. 1). Utilizing the adjusted dataset, a comprehensive database was established comprising 100 training points derived from the VIs values obtained from selected pixels across months of interest, within a total of 40 parcels.

$$\text{Normalized} = \frac{\text{Indices-Indices(min)}}{\text{Indices (max) -Indices(min)}} \quad (1)$$

The phenology of winter wheat is divided into four distinct phases: seeding-germination, tillering-jointing, heading-blooming, and maturity-harvesting (Mashonganyika et al., 2021; Zhou et al., 2022) (Table 2 and Figure 4). In this investigation, a time series graph was generated from the calculated VIs (Figure 4), which allowed for the correlation of the VIs time series with a variety of phenological phases, thereby facilitating the characterization of winter wheat phenology stages (Mashonganyika et al., 2021).

Table 1. Cadastral and yield information of selected parcels.

Number of Parcels	Block	Parcel No	Area (da)	Province	City	Neighborhood	Land Use	Yield(da)
1	121	1	15330,28	Çanakkale	Center	Halileli	Cultivated	300
2	119	10	24666,84	Çanakkale	Center	Halileli	Cultivated	400
3	121	50	18084,94	Çanakkale	Center	Halileli	Cultivated	500
4	121	51	7091,41	Çanakkale	Center	Halileli	Cultivated	500
5	121	52	5733,59	Çanakkale	Center	Halileli	Cultivated	450
6	145	19	86948,03	Çanakkale	Center	Halileli	Cultivated	550
7	145	20	31684,74	Çanakkale	Center	Halileli	Cultivated	450
8	105	35	26036,05	Çanakkale	Center	Halileli	Cultivated	500
9	174	4	5562,08	Çanakkale	Center	Kumkale	Cultivated	600
10	172	87	10264,67	Çanakkale	Center	Kumkale	Cultivated	550
11	176	3	14454,31	Çanakkale	Center	Kumkale	Cultivated	700
12	146	4	34668,2	Çanakkale	Center	Kumkale	Cultivated	775
13	113	29	6603,91	Çanakkale	Center	Kumkale	Cultivated	1200
14	113	28	3719,82	Çanakkale	Center	Kumkale	Cultivated	1100
15	113	27	3657,19	Çanakkale	Center	Kumkale	Cultivated	1000
16	113	26	9919,89	Çanakkale	Center	Kumkale	Cultivated	1100
17	113	25	17419,04	Çanakkale	Center	Kumkale	Cultivated	1100
18	115	33	4867,09	Çanakkale	Center	Kumkale	Cultivated	1250
19	115	32	7439,64	Çanakkale	Center	Kumkale	Cultivated	1100
20	115	31	14300,16	Çanakkale	Center	Kumkale	Cultivated	1100
21	115	30	6500,07	Çanakkale	Center	Kumkale	Cultivated	1000
22	117	9	26049,1	Çanakkale	Center	Kumkale	Cultivated	900
23	238	26	12006,24	Çanakkale	Center	Kumkale	Cultivated	1000
24	238	27	3630,5	Çanakkale	Center	Kumkale	Cultivated	1000
25	238	28	2585,48	Çanakkale	Center	Kumkale	Cultivated	1000
26	238	57	5334,4	Çanakkale	Center	Kumkale	Cultivated	1050
27	238	58	2229,13	Çanakkale	Center	Kumkale	Cultivated	1050
28	238	59	11157,57	Çanakkale	Center	Kumkale	Cultivated	1050
29	238	137	30407,45	Çanakkale	Center	Kumkale	Cultivated	1025
30	117	4	3754	Çanakkale	Center	Kalafat	Cultivated	1050
31	117	5	3577	Çanakkale	Center	Kalafat	Cultivated	1050
32	117	6	4072	Çanakkale	Center	Kalafat	Cultivated	1050
33	132	25	27852,92	Çanakkale	Center	Ciplak	Cultivated	900
34	196	49	32436,92	Çanakkale	Center	Ciplak	Cultivated	825
35	196	80	2501,26	Çanakkale	Center	Ciplak	Cultivated	850
36	196	88	3045,67	Çanakkale	Center	Ciplak	Cultivated	900
37	196	87	3656,57	Çanakkale	Center	Ciplak	Cultivated	1000
38	196	86	12158,97	Çanakkale	Center	Ciplak	Cultivated	1000
39	-	124	4507	Çanakkale	Ezine	Pinarbasi	Cultivated	900
40	-	123	8309	Çanakkale	Ezine	Pinarbasi	Cultivated	800

Upon analyzing the normalized VIs values within the time series, it was observed that the lowest values occurred during the first week of December, as well as in January and February. These relationships are consistent with the seeding-germination stage of winter wheat growth, indicating a direct relationship between the normalized VIs and the

Table 2. Characteristics of satellite imagery used for VIs and phenological stages.

LANDSAT 8-9 OLI- TIRS				
Sensor/Platform	Date	Resolution (m)	Cloud-free rate (%)	Phenological Stage
LANDSAT/LC08/C02/T1_TOA	44916	30	40	Seeding-Germination
LANDSAT/LC08/C02/T1_TOA	44971	30	20	Tillering-Jointing
LANDSAT/LC08/C02/T1_TOA	45012	30	20	Tillering-Jointing
LANDSAT/LC09/C02/T1_TOA	45036	30	46,41	Heading-Blooming
LANDSAT/LC09/C02/T1_TOA	45059	30	20	Heading-Blooming
LANDSAT/LC09/C02/T1_TOA	45091	30	20	Maturity-Harvesting

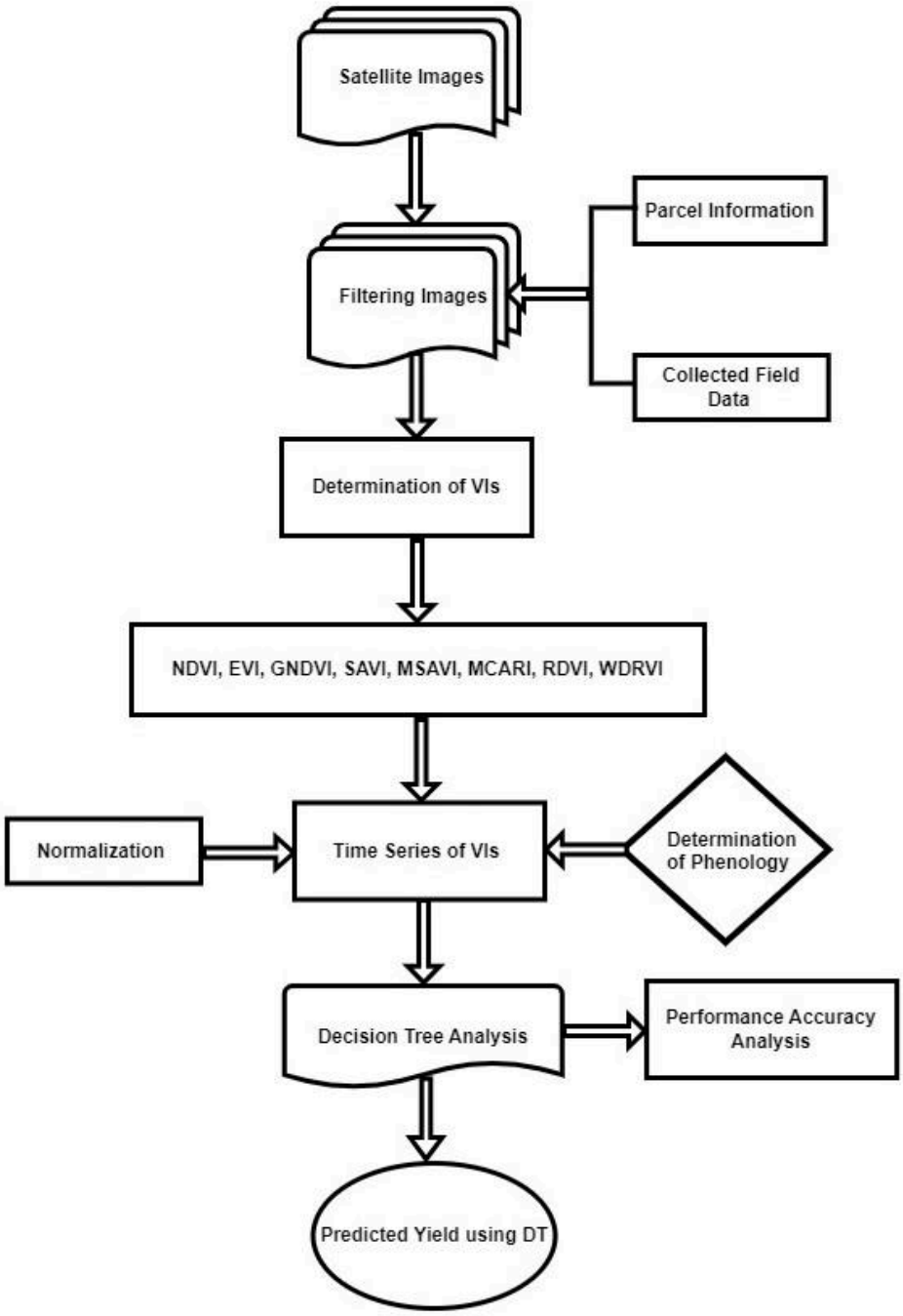

Figure 3. Flow chart of the study.

Table 3. VIs used to predict winter wheat yield prediction.

Vegetation Index	Equations	References
NDVI	$\mathrm{NDVI} = \frac{\mathrm{NIR} - \mathrm{RED}}{\mathrm{NIR} + \mathrm{RED}}$	Deng et al., (2022)
EVI	$\mathrm{EVI} = G * [((\mathrm{NIR} - \mathrm{RED}))/ (\mathrm{NIR} + C1 * \mathrm{RED} - C2 * \mathrm{BLUE} + L)]$	Saad El Imanni et al., (2022)
GNDVI	$\mathrm{GNDVI} = \mathrm{NIR}$ - Green / $\mathrm{NIR} +$ Green	Jamali et al., (2023)
RDVI	$\mathrm{RDVI} = (\mathrm{NIR} - \mathrm{RED}) / (\mathrm{NIR} + \mathrm{RED})$	Segarra et al., (2020)
SAVI	$\mathrm{SAVI} = (\mathrm{NIR}$ - $\mathrm{RED})/(\mathrm{NIR} + \mathrm{RED}) + L\ X\ (1 + L)$	Skendzic et al., (2023)
MSAVI	$\mathrm{MSAVI} = 2x\ \mathrm{NIR} + 1 - \mathrm{sqrt}()\ (2x\ \mathrm{NIR} + 1)2 - 8(\mathrm{NIR} - \mathrm{Red}))/2$	Liu et al., (2022)
MCARI	$\mathrm{MCARI} = ((\mathrm{NIR} - \mathrm{RED}) - 0.2\ (\mathrm{NI} -\ \mathrm{GREEN}))x\ (\mathrm{NIR}\ /(\mathrm{RED}))$	Zhen et al., (2020)
WDRVI	$\mathrm{WDRVI} = 0.1\ x\frac{\mathrm{NIR} - \mathrm{RED}}{\mathrm{NIR} + \mathrm{RED}}$	Naqvi et al., (2018)

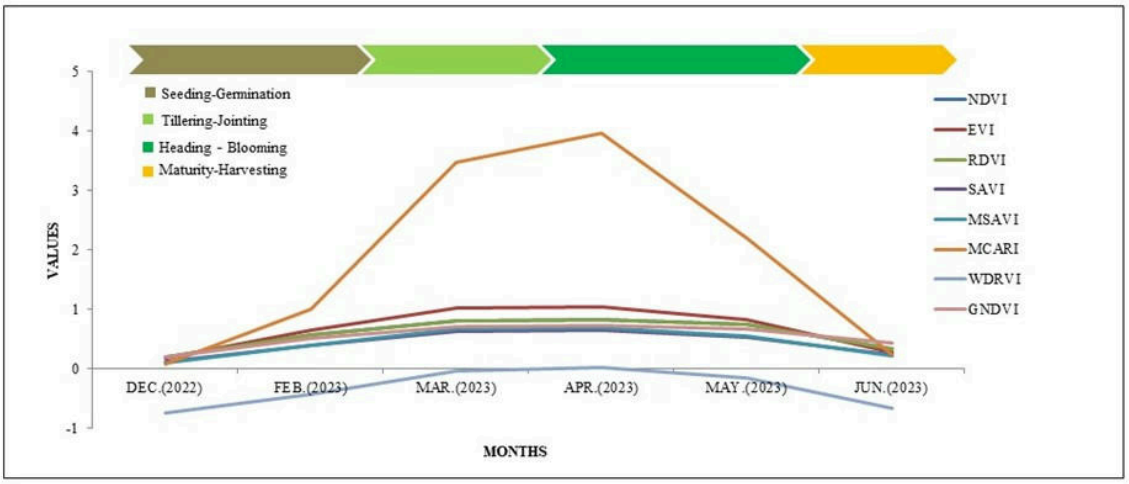

Figure 4. Normalized VI monthly average values and phenological period.

corresponding phenological stage. The end of February and March represent the tillering-jointing stage and winter wheat reaches its greenest form at heading-blooming stage end of March and April, and the VIs values were at their highest (Khan et al., 2023). Therefore, the months of April and mid-May, when VIs reach the highest value, are considered the heading-blooming stage. After the heading-blooming stage, maturity-harvesting, winter wheat begins to take on a yellowish color (Campos et al., 2019). During this stage, winter wheat does not display a healthy plant characteristic as it did during the heading-blooming stages, and values of VIs began to decrease. The time series graph of VIs values for the winter wheat plant in study area for the 2022-2023 season is given Figure 4.

Decision Tree Classification

A database was created to develop an early yield prediction model for winter wheat fields. This process involved processing images using GEE, calculating VIs to determine time series data, and obtaining real yield values as described earlier. To construct a predictive model, C4.5 DT classification algorithms were utilized to develop methods for classifying VIs values based on actual yield. The results of the C4.5 DT classification algorithms were analyzed to determine the month in which they could predict 'Low Yield,' 'Medium Yield,' and 'High Yield' in different phenology stages. Furthermore, the development of C4.5 DT algorithms and the evaluation of their performance accuracy were carried out. When the studies conducted based on previous classifiers for classification methods in knowledge acquisition were examined, it was observed that algorithms with high detection rates and low false alarm rates were C4.5 DT and RF (Chauhan et al., 2013; Mallissery et al., 2013; Aggarwal and Sharma, 2015). Furthermore, visualizing the trees produced assistance in comprehension alongside studying, and both numerical and categorical data can be analyzed through the C4.5 DT algorithm (Gupta et al., 2017). Consequently, the C4.5 DT information retrieval algorithm was selected for this research. The prediction model for calculating winter wheat parcel yield values based on VIs was established using the C4.5 DT algorithm within RapidMiner Studio software (Yucebas et al., 2022).

VIs time series values were used as numerical data, while yield values were used as categorical data (Table 4). For the

categorical data set, the unit value was divided into three classes: 'Low Yield,' 'Medium Yield,' and 'High Yield.' Values between 300 and 552 were categorized as low, values between 553 and 1117 were categorized as medium, and values between 1118 and 1250 were categorized as high in the specified classes. The formulas provided below were utilized in determining the class labels Eq. (2-4) (Yucebas et al., 2022).

$$\text{Low} = [\ \text{MinUnit\_Yield}\ ,\ \ \text{MinUnit\_yield} + \sigma] \quad (2)$$

$$\text{Medium} = [\ \text{MinUnit\_Yield} + \sigma{+}1,\ \bar{x}{+}\ \sigma] \quad (3)$$

$$\text{High} = [\bar{x}{+}\ \sigma{+}1,\ \ \text{MaxUnit\_Yield}\ ] \quad (4)$$

Standard deviation *(σ)* and mean *($\bar{x}$)* were used for the value range. The depths of the created trees were set to 10 (Table 4). A pruning algorithm was employed to minimize repeated paths. It was observed that the 'Gini Index' tree type exhibited the highest accuracy in classification in the study (Cai et al., 2010). Therefore, it was chosen for use in the study.

Results

Prediction of the Winter Wheat Yield – Vis

In the assessment of performance accuracy for the C4.5 DT algorithm, the predictive capacity of individual indices was analyzed using a data subset comprising 10% or more of the entire dataset. Upon examining the yield prediction results presented in Figure 5 and Table 4, C4.5 DT models demonstrated a classification accuracy of 97,50% in April, which is critical for the prediction of the yield for the study area in the 2023 season. It was noticed that C4.5 DT was able to accurately predict the yield of parcels by categorizing NDVI values, and it was found that April is a crucial month for NDVI. If the NDVI value is less than or equal to 0,913, the parcel yield will be predicted as 'Low Yield' (300-552 kg/da). If the NDVI value is greater than 0,913, the NDVI values for April will be reevaluated. In the second node of the DT, if the NDVI value is greater than 0,925, the parcel yield is predicted as 'High Yield' (1118-1250 kg/da). Otherwise, the parcel yield will be predicted as 'Medium Yield' (553-1117 kg/da).

The C4.5 DT model resulted that April as the critical time for yield prediction with a classification accuracy of 77,50%. According to this, the yield can be estimated as 'Low Yield' parcels when EVI is less than or equal to 1,010 in April. If EVI is greater than 1,010, the values of March were checked and EVI is greater than 1,071, parcel yield is predicted as 'High Yield'. If EVI value is less than or equal to 1,071, the EVI value of June should be checked. In June, when EVI is less than or equal to 0,068, a decision could not be made, and control was carried out in May. In May, when EVI is greater than 0,923, in February when EVI is greater than 0,725, parcels with 'Medium Yield' were predicted (Figure 5). Similarly, GNDVI also determined April as the critical time for predicted yield with an 87,50% accuracy. In April, if GNDVI is greater than or equal to 0,863, it is predicted as 'Low Yield'. If GNDVI is less than or equal to 0,875, the parcel is predicted as 'Medium Yield,' and if GNDVI is greater than 0,875, GNDVI values for the December node should be checked. In the December node, if GNDVI is less than 0,650, the April node is reevaluated. Greater than 0,877 in April, the parcel is predicted as 'High Yield' for GNDVI. In April, the starting note was identified as having 97,50% accuracy for the RDVI classification. If the RDVI value in April is equal to or less than 0,913, it is predicted as 'Low Yield.' If the RDVI value is greater than 0,913, the values are reevaluated in April, and if the RDVI value is equal to or less than 0,925, it is predicted as "Medium Yield." If the RDVI value is greater than 0,925 in April, 'High Yield' parcels can be predicted (Figure 5). Furthermore, the analysis showed that MSAVI had a classification accuracy of 82,50% in April. When MSAVI is less than or equal to 0,836, the parcel is predicted as 'Low Yield'. If MSAVI is less than or equal to 0,865, the parcel is predicted as 'Medium Yield,' and if MSAVI is greater than 0,865, then the MSAVI value from the February node is examined. The MSAVI value is greater than 0,588, the MSAVI value from April is reevaluated, and parcels with MSAVI values over 0,873 are predicted as 'High Yield' (Figure 5). The results indicated that April also played a significant role in predicting winter wheat yield using the MCARI, with an accuracy rate of 85,0%. When the MCARI index is analyzed, April also played a significant role in predicting winter wheat yield using the MCARI, with an accurate rate of 85,0% (Table 4). If the MCARI value was equal to or less than 2,336 in April, it was classified as 'Low Yield.' If the MCARI value was greater than 2,336 but less than or equal to 2,931 in April, the parcel indicates "Medium Yield". The MCARI value was greater than 2,931 in April, then the values for the March node were examined. The MCARI value in March was greater than 1,871, it could indicate 'High Yield' parcels. The analysis revealed that April is a crucial period for predicting winter wheat yield using the WDRVI index with 97,50% accuracy. In April, if the WDRVI is less than or equal to 0,510, the parcel was classified as 'Low Yield'. If the WDRVI was greater than 0,510, it should be reassessed in April. Furthermore, if the WDRVI was less than or equal to 0,550 in April, it was classified as 'Medium Yield', while a value greater than 0,550 indicated 'High Yield' for the parcels (Figure 5). The SAVI index, with a classification accuracy of 75,0%, also indicated that April is the most important period to predicted wheat yield (Table 4). It was determined that if the SAVI value was equal to or lower than 0,815 in April, the parcel was predicted as a 'Low Yield.' However, the SAVI value was greater than 0,815 in April, further examination was required. In this case, the SAVI value was less than or equal to 0,843 in the December node, the parcel was

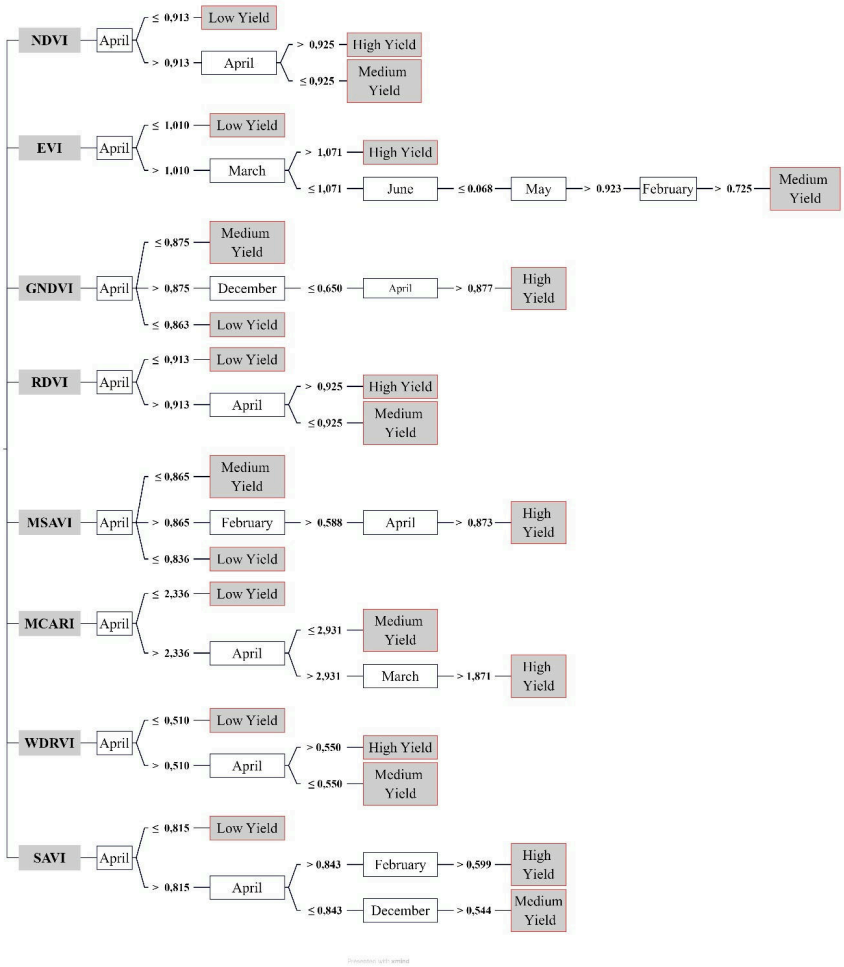

Figure 5. Combination of sub-decision trees for yield prediction of vegetation indices.

Table 4. Performance accuracy values of winter wheat yield prediction based on C4.5-DT.

Tree Name	Performance Accuracy Analysis (%)	Month of best prediction 'Low Yield'	Month of best prediction 'Medium Yield'	Month of best prediction 'High Yield'
NDVI	97,50	April	April	April
EVI	77,50	April	February	March
GNDVI	87,50	April	April	April
RDVI	97,50	April	April	April
MSAVI	82,50	April	April	April
MCARI	85,00	April	April	April
WDRVI	97,50	April	April	April
SAVI	75,00	April	December	February

predicted to have a 'Medium Yield'. Moreover, if the SAVI value was greater than 0,544 in December, a 'Medium Yield' parcel was predicted. Additionally, it was observed that parcels were identified as 'High Yield' if the SAVI value was higher than 0,843 in April and greater than 0,599 in February (Figure 5).

All VIs generated from Landsat 8-9 data can be used to predict 'Low Yield' in April, which is the heading-blooming period of winter wheat. Additionally, 'Medium Yield' can be predicted in April using NDVI, GNDVI, RDVI, MACARI, MSAVI, and WDRVI, but EVI in February and SAVI in December. Furthermore, EVI can predict 'High Yield' parcels in March, which is the tillering-jointing period of winter wheat phenology, and SAVI can forecast 'High Yield' in February, marking the end of the seeding-germination period (Table 4, Figure 5). All other VIs also predicted 'High Yield' in April.

Discussion and Conclusion

This study aimed to find the best times to predict 'Low Yield,' 'Medium Yield,' and 'High Yield' areas by looking at the VIs of winter wheat during its growth stages and using the C4.5 DT classification algorithm. Overall findings indicated that April is a critical month for yield prediction during the heading-blooming stages. During this time, yield predictions made using the NDVI, EVI, GNDVI, RDVI, MSAVI, MCARI, WDRVI, and SAVI indices showed high accuracy rates between 75.50% and 97.50%. It has been shown in research that April is a good time to predict winter wheat yield using RS data in semi-arid regions, especially during the heading-blooming stage. Similarly, Song et al. (2016) stated that the use of Landsat 8-derived NDVI during the heading-blooming stage for predicting winter wheat yield is valuable information for agricultural sectors. The results of our study are consistent with similar studies in literature (Castaldi et al., 2015; Song et al., 2016; Ma et al., 2022; Newete et al., 2024; Xiao et al., 2024; Du et al., 2025; Raza et al., 2025). Ma et al. (2022) mentioned that using the Simple Yield Prediction Algorithm (SAFY) model, which combines RS data and biomass data at the beginning of the blooming period, is important for predicting yield because key factors are at their peak during this time. Although the model is different, we have found a comparable result.

Similarly, in a supporting study by Newete et al. (2024), the optimum suitable period for yield forecast in South Africa was discovered to be the heading -blooming phase of wheat prediction. This study also reveals that the ideal time to estimate wheat output in northwest Turkey is the heading-blooming period, more notably, the peak flowering phase in April. The overall results of the research suggest that VIs can independently of climatic data highlight physiological and structural changes in plants. Independent of climate data, this condition has revealed the remarkable precision with which VIs can identify wheat phenological stages. By means of a R^2 value of 0.77 using the Multiple Linear Regression model (Faqe Ibrahim et al., 2023), this method validates earlier studies showing a good correlation between wheat yield and VIs from Landsat 8. This paper reveals that simply VIs enable one to precisely project the winter wheat output without integrating climate data such temperature, precipitation, and Growing Degree Days (GDD). The outcome suggests that, provided the plants are healthy and free from diseases, elements like temperature, rainfall, and sunlight influence how well a plant develops; so, using VIs helps one to estimate growth and yield using only RS-based VIs. This result implies that we should create simpler models using just RS data as a substitute and that the link between VIs and projecting wheat yield might be stronger than we thought. Segarra et al. (2020) also found that the heading-blooming stage in April is the optimal time to anticipate winter wheat yield using climate factors (such as precipitation, temperature, and GDD) paired with RDVI (R^2 = 0.84) and MSAVI (R^2 = 0.83).

Ashfaq et al. (2024), who claimed that the use of just VIs can help in the prediction of wheat yield, validated our results. Their study showed that more accurate forecasts (R^2 = 0.78–0.88) arise from the combination of climate and RS data than from models based just on restricted data (R^2 = 0.65–0.732) or RS data (R^2 = 0.49–0.70). Without using any climate data, this study generated extremely accurate predictions for "High Yield" winter wheat in April using NDVI (97.50%), GNDVI (87.50%), RDVI (97.50%), MSAVI (82.50%), MCARI (85.00%), and WDRVI (97.50%). Using an ML technique known as C4.5-DT While SAVI (75.50%) expected this in the early stages of seeding-germination (December), EVI (77.5%) expected "High Yield" throughout the seeding-germination (February) phases. Thayanandeswari et al. (2024) examined how effectively multiple ML approaches, including SVM, DT, and RF, may predict crop production using vegetation indices and climate data. With an accuracy of 98% and more constant forecasts of wheat yield, the DT-RF algorithm was the best. Research on using VIs with ML found that the XGBoost and RF models considerably improved prediction accuracy, with scores of R^2 = 0.81 and R^2 = 0.60. Based on these studies, simply using VIs yields accuracy rates between 75.50% and 97.50% and the C4.5-DT-based model is a good and dependable way to anticipate wheat output. Unlike simpler DT and other ML methods, the results indisputably reveal that for limited areas integrating RS data with the C4.5 -DT model produces rather accurate yield projections. The use of climate data remains limited, despite its capacity to alleviate challenges related to the continuous monitoring of plots.

This difference is important because satellite imagery allows for a comprehensive assessment of the effects of climate on plant characteristics. It was developed a rapid, cost-effective, and simple method for predicting agricultural yields during the phenological mid-stages, which aligns with the United Nations Sustainable Development Goal 2, "Zero Hunger." A C4.5-DT-based ML model using only RS data indicates that April is a critical time for predicting winter wheat production in northern Turkey. Title: Flowering periods can vary significantly depending on the physical characteristics of different countries (elevation, location, topography, etc.) and should be recognized as an important tool not only for Türkiye but also for assessing the adequacy of global winter wheat stocks. The independent use of RS allows researchers and practitioners to improve yield predictions, which facilitates access to information, especially in regions

where traditional data collection, such as climate data, is difficult. We encourage the use of high-resolution satellite images, surface temperatures, and images obtained from VIs as effective tools for covering large areas, which facilitates the faster assessment of agricultural conditions. The study's results indicate that RS-based VIs are accurate and reliable compared to C4.5-DT-based ML methods, indicating that there is room for enhancements in future research. Future studies should integrate environmental variables such as climate data and soil properties, evaluate the model using extended datasets, and adapt it for other scales and contexts. By using the appropriate VIs and ML methods along with thorough research, we can create models that consider environmental factors, which will help us better analyze agricultural productivity. Future studies could enhance its effectiveness by examining the applicability of this approach to different crops and locations. In summary, this study demonstrates that yield predictions obtained solely from VIs are accurate and shows the impact of external factors such as weather on plant health.

Acknowledgements	The authors would like to express their gratitude to the ComAgEnPlan working group individuals for data collection in the field.
Peer Review	Externally peer-reviewed.
Author Contributions	Conception/Design of Study: L.G..; Data Acquisition- N.C., L.G.; Data Analysis/Interpretation N.C., L.G.; Drafting Manuscript- N.C., L.G.; Critical Revision of Manuscript- L.G., Ö.A..; Final Approval and Accountability- N.C., L.G., Ö.A.
Conflict of Interest	Authors declared no conflict of interest.
Financial Disclosure	Authors declared no financial support.

Author Details

Neslihan Civelek

[1] Çanakkale Onsekiz Mart University, Department of Geographic Information Technologies, Çanakkale, Türkiye

0009-0007-6077-7689

Levent Genç

[2] Çanakkale Onsekiz Mart Üniversitesi, Faculty of Architecture and Design, Department of Urban and Regional Planning, Çanakkale, Türkiye

0000-0002-0074-0987 leventgc@comu.edu.tr

Özgün Akçay

[3] Çanakkale Onsekiz Mart University, Geomatic Engineering, Çanakkale, Türkiye

0000-0003-0474-7518

REFERENCES

Adeniyi, D.O., Szabo, A., Tama, J., Nagy, A. (2020). Winter wheat yield forecasting is based on Landsat NDVI and SAVI time series. https://doi.org/10.20944/preprints202007.0065.v

Aggarwal, P., Sharma, S.K. (2015). An empirical comparison of classifiers to analyze intrusion detection. *International Conference on Advanced Computing and Communication Technologies*, 446–450. https://doi.org/10.1109/ACCT.2015.59

Aghlmand, M., Kalkan, K., Onur, M.I., Öztürk, G., Ulutak, E. (2021). Google Earth Engine ile arazi kullanımı haritalarının üretimi. *Ömer Halisdemir University Journal of Engineering Sciences*, 10(1), 038-047. https://doi.org/10.28948/ngumuh.795977

Ashfaq, M., Khan, I., Alzahrani, A., Tariq, M. U., Khan, H., & Ghani, A. (2024). Accurate wheat yield prediction using machine learning and climate-NDVI data fusion. *IEEE Access, 12*, 40947–40961. https://doi.org/10.1109/ACCESS.2024.3376735

Ayub, M., Khan, N.A., Haider, R.Z. (2022). Winter wheat crop field and yield prediction using remote sensing and machine learning. *2nd IEEE International Conference on Artificial Intelligence (ICAI)*, 158–164. https://doi.org/10.1109/ICAI55435.2022.9773663

Bebie, M., Cavalaris, C., Kyparissis, A. (2022). Assessing durum winter wheat yield through Sentinel-2 imagery: A machine learning approach. *Remote Sensing Sciences*, 14(16). https://doi.org/10.3390/rs14163880

Bouras, E. houssaine, Olsson, P. O., Thapa, S., Díaz, J. M., Albertsson, J., & Eklundh, L. (2023). wheat yield estimation at high spatial resolution through the assimilation of Sentinel-2 data into a crop growth model. *Remote Sensing*, 15(18). https://doi.org/10.3390/rs15184425

Cai, W.T., Liu, Y.X., Li, M.C., Zhang, Y., Li, Z. (2010). The best-first multivariate decision tree method used for urban land cover classification.

Campos, I., Gonzalez, G.L., Villodre, J., Calera, M., Campoy, J., Jimenez, N., Plaza, C., Sanchez, P.S., Calera, A. (2019). Mapping within-field variability in winter wheat yield and biomass using remote sensing vegetation indices. *Precision Agriculture*, 20(2), 214–236. https://doi.org/10.1007/s11119-018-9596-z

Castaldi, F., Casa, R., Pelosi, F., & Yang, H. (2015). Influence of acquisition time and resolution on wheat yield estimation at the field scale from canopy biophysical variables retrieved from SPOT satellite data. *International Journal of Remote Sensing*, *36*(9), 2438–2459. https://doi.org/10.1080/01431161.2015.1041174

Cavalaris, C., Megoudi, S., Maxouri, M., Anatolitis, K., Sifakis, M., Levizou, E., & Kyparissis, A. (2021). Modeling of durum winter wheat yield based on sentinel-2 imagery, *Agronomy,* 11(8). https://doi.org/10.3390/agronomy11081486

Chauhan, H., Kumar, V., Pundir, S., Pilli, E.S. (2013). A comparative study of classification techniques for intrusion detection. *Proceedings 2013 International Symposium on Computational and Business Intelligence (ISCBI)*, 40–43. https://doi.org/10.1109/ISCBI.2013.16

Cheng, E., Zhang, B., Peng, D., Zhong, L., Yu, L., Liu Y, Xiao C, Li C, Li X, Chen Y, Ye H, Wang H, Yu R, Hu J, & Yang S (2022). Winter wheat yields estimation using remote sensing data based on machine learning approaches. *Frontiers in Plant Science,* 13. https://doi.org/10.3389/fpls.2022.1090970

Deng, S., Gao, M., Ren, C., Li, S., Liang, Y. (2022). Extraction of sugarcane planting area based on similarity of NDVI time series. *IEEE Access*, 10, 117362–117373. https://doi.org/10.1109/ACCESS.2022.3219841

Du, X., Zhu, J., Xu, J., Li, Q., Tao, Z., Zhang, Y., Wang, H., & Hu, H. (2025). Remote sensing-based winter wheat yield estimation integrating machine learning and crop growth multi-scenario simulations. *International Journal of Digital Earth*, 18(1). https://doi.org/10.1080/17538947.2024.2443470

Faqe Ibrahim, G. R., Rasul, A., & Abdullah, H. (2023). Sentinel-2 accurately estimated wheat yield in a semi-arid region compared with Landsat 8. *International Journal of Remote Sensing*, 44(13), 4115–4136. https://doi.org/10.1080/01431161.2023.2232542

Genc, L., Turhan, H., Asar, B., & Smith, S. (2009). Comparision of spectral indices derived from QICKBIRD and ground based hyper-spectral data for winter wheat. *World Applied Sciences Journal*, 7, 756-762.

Genc, L., Demirel, K., Çamoğlu, G., Aşık, S., Smith, S. (2011). Determination of plant water stress using spectral reflectance measurements in watermelon (Citrullus vulgaris). *American-Eurasian J. Agric. & Environ. Sci.*, 11(2), 296-304.

Goldberg, K., Herrmann, I., Hochberg, U., & Rozenstein, O. (2021). Generating up-to-date crop maps optimized for Sentinel-2 imagery in Israel. *Remote Sensing*, 13(17). https://doi.org/10.3390/rs13173488

Gupta, B., Uttarakhand, P., Rawat, I.A. (2017). Analysis of various decision tree algorithms for classification in data mining. *International Journal of Computer Applications*, 163(8), 0975-8887.

Inalpulat, M., Genc, L. (2019). Monitoring short term seasonal changes in wetlands: Aremote sensing study of Kumkale, Çanakkale (Türkiye). *International Symposium on Biodiversity Research*.

Jamali, M., Bakhshandeh, E., Yeganeh, B., & Özdoğan, M. (2023). Development of machine learning models for estimating winter wheat biophysical variables using

satellite-based vegetation indices. *Advances in Space Research*, 73(1), 498–513. https://doi.org/10.1016/j.asr.2023.10.004

Khan, H. R., Gillani, Z., Jamal, M. H., Athar, A., Chaudhry, M. T., Chao, H., He, Y., & Chen, M. (2023). Early identification of crop type for smallholder farming systems using deep learning on time series Sentinel 2 imagery. *Sensors Science*, 23(4). https://doi.org/10.3390/s23041779

Khechba, K., Belgiu, M., Laamrani, A., Stein, A., Amazirh, A., & Chehbouni, A. (2025). The impact of spatiotemporal variability of environmental conditions on wheat yield forecasting using remote sensing data and machine learning. *International Journal of Applied Earth Observation and Geoinformation*, 136. https://doi.org/10.1016/j.jag.2025.104367

Kobayashi, N., Tani, H., Wang, X., Sonobe, R. (2020). Crop classification using spectral indices derived from Sentinel 2A imagery. *Journal of Information and Telecommunication,* 4(1), 67–90. https://doi.org/10.1080/24751839.2019.1694765

Liu, S., Peng, D., Zhang, B., Chen, Z., Yu, L., Chen, J., Pan, Y., Zheng, S., Hu, J., Lou, Z., Chen, Y., Yang, S. (2022). The accuracy of winter winter wheat identification at different growth stages using remote sensing. *Remote Sensing,* 14(4). https://doi.org/10.3390/rs14040893

Ma, C., Liu, M., Ding, F., Li, C., Cui, Y., Chen, W., & Wang, Y. (2022). Wheat growth monitoring and yield estimation based on remote sensing data assimilation into the SAFY crop growth model. *Scientific Reports*, 12(1). https://doi.org/10.1038/s41598-022-09535-9

Mallissery, S., Kolekar, S., & Ganiga, R. (2013). Accuracy analysis of machine learning algorithms for intrusion detection system using NSL-KDD dataset. https://doi.org/10.13140/RG.2.1.5018.0247

Mashonganyika, F., Mugiyo, H., Svotwa, E., & Kutywayo, D. (2021). Mapping of winter winter wheat using Sentinel-2 NDVI data a case of Mashonaland Central Province in Zimbabwe. *Frontiers in Climate,* 3. https://doi.org/10.3389/fclim.2021.715837

Memon, M. S., Chen, S., Niu, Y., Zhou, W., Elsherbiny, O., Liang, R., Du, Z., Guo, X. (2023). Evaluating the efficacy of Sentinel-2B and Landsat-8 for estimating and mapping winter wheat straw cover in rice winter wheat fields. *Agronomy,* 13(11). https://doi.org/10.3390/agronomy13112691

Nagy, A., Szabo, A., Adeniyi, O. D., Tamas, J. (2021). Winter wheat yield forecasting for the Tisza River catchment using Landsat 8 NDVI and SAVI time series and reported crop statistics. *Agronomy,* 11(4). https://doi.org/10.3390/agronomy11040652

Navada, A., Ansari, A. N., Patil, S., & Sonkamble, B. A. (2011). Overview of use of decision tree algorithms in machine learning. *In 2011 IEEE Control and System Graduate Research Colloquium,* Department of Computer Engineering, Pune Institute of Computer Technology, Pune, India.

Naqvi, S. M. Z. A., Tahir, M. N., Shah, G. A., Sattar, R. S., Awais, M. (2018). Remote estimation of winter wheat yield based on vegetation indices derived from time series data of Landsat 8 imagery. *Applied Ecology and Environmental Research,* 17(2), 3909–3925. https://doi.org/10.15666/aeer/1702_39093925

Newete, S. W., Abutaleb, K., Chirima, G. J., Dabrowska-Zielinska, K., & Gurdak, R. (2024). Phenology-based winter wheat classification for crop growth monitoring using multi-temporal Sentinel-2 satellite data. *Egyptian Journal of Remote Sensing and Space Science*, 27(4), 695–704. https://doi.org/10.1016/j.ejrs.2024.10.001

Panda, S. S., Ames, D. P., & Panigrahi, S. (2010). Application of vegetation indices for agricultural crop yield prediction using neural network techniques. *Remote sensing*, 2(3), 673-696.

Purwanto, A.D., Wikantika, K., Deliar, A., Darmawan, S. (2022). Decision tree and random forest classification algorithms for mangrove forest mapping in Sembilang National Park Indonesia. *Remote Sensing,* 15(1). https://doi.org/10.3390/rs15010016

Qi, X., Wang, Y., Peng, J., Zhang, L., & Yuan, W. (2022). The 10-meter winter winter wheat mapping in Shandong province using Sentinel-2 data and coarse resolution maps. *IEEE Journal of Selected Topics in Applied Earth Observations and Remote Sensing*, 15, 9760–9774. https://doi.org/10.1109/JSTARS.2022.3220698

Saad El Imanni, H., El Harti, A., & El Iysaouy, L. (2022). Winter wheat yield estimation using remote sensing indices derived from Sentinel-2 time series and Google Earth Engine in a highly fragmented and heterogeneous agricultural region. *Agronomy,* 12(11). https://doi.org/10.3390/agronomy12112853

Segarra, J., Gonzalez Torralba, J., Aranjuelo, I., Araus, J. L., & Kefauver, S. C. (2020). Estimating winter wheat grain yield using Sentinel-2 imagery and exploring topographic features and rainfall effects on winter wheat performance in Navarre, Spain. *Remote Sensing,* 12(14). https://doi.org/10.3390/rs12142278

Skakun, S., Franch, B. E., Vermote, J. C., Roger, C., Justice, J., Masek, E., & Murphy. (2018). Winter winter wheat yield assessment using Landsat 8 and Sentinel-2 data. *In Proc. 2018 IEEE International Geoscience and Remote Sensing Symposium (IGARSS),* Valencia, Spain.10.1109/IGARSS.2018.8518885

Esfandabadi, H. S., Asl, G.M., Esfandabadi, Z. S., Gautam, S., & Ranjbari, M. (2021). Drought assessment in paddy rice fields using remote sensing technology towards achieving food security and SDG2. *British Food Journal,* 124(12), 4219–4233. https://doi.org/10.1108/BFJ-08-2021-0872

Sharma, R., Ghosh, A., & Joshi, P. K. (2013). Decision tree approach for classification of remotely sensed satellite data using open-source support. *Earth System Science,* 122(5), 1237-1247.

Skendzic, S., Zovko, M., Lesic, V., Pajac, Z. I., Lemic, D. (2023). Detection and evaluation of environmental stress in winter winter wheat using remote and proximal sensing methods and vegetation indices a review. *Diversity (MDPI),* 15(481). https://doi.org/10.3390/d15040481

Song, R., Cheng, T., Yao, X., Tian, Y., Zhu, Yan., Cao, & Weixing. (2016, July). Evaluation of Landsat 8 time series image stacks for predicting yield and yield components of winter wheat. *2016 IEEE International Geoscience & Remote Sensing Symposium.* Beijing, China.

Syamala, D. M., Guleria, A., & Rai, K. (2016). Decision tree based algorithm for intrusion detection. *International Journal of Advenced Networking and Applications,* 7(4), 2828-2834.

Thayanandeswari, C. S. S., Jaya, T., Ahamed, S. N., Bommy, B., Kumar, G. B., & Shyjith, M. B. (2024). A machine learning approach for crop yield prediction using weather condition. *Proceedings of the 2024 International Conference on Advancement in Renewable Energy and Intelligent Systems, AREIS 2024.* https://doi.org/10.1109/AREIS62559.2024.10893606

Thieme, A., Yadav, S., Oddo, P. C., Fitz, J. M., McCartney, S., King, L. A., Keppler, J., McCarty G. W., & Hively, W. D. (2020). Using NASA Earth Observations and Google Earth Engine to map winter cover crop conservation performance in the Chesapeake Bay watershed. *Remote Sensing of Environment,* 248. https://doi.org/10.1016/j.rse.2020.111943

Toscano, P., Castrignano, A., Di Gennaro, S. F., Vonella, A. V., Ventrella, D., & Matese, A. (2019). A precision agriculture approach for durum winter wheat yield assessment using remote sensing data and yield mapping. *Agronomy,* 9(8). https://doi.org/10.3390/agronomy9080437

Peng, D., Cheng, E., Feng, X., Hu, J., Lou, Z. H., Zhao, B., Lv, Y., Peng, H., & Zhang, B. (2024). A deep–learning network for wheat yield prediction combining weather forecasts and remote sensing data. *Remote Sensing*, *16*(19). https://doi.org/10.3390/rs16193613

Virtriana, R., Riqqi, A., Anggraini, T. S., Fauzan, K. N., Ihsan, K. T. N., Mustika, F. C., Suwardhi, D., Harto, A. B., Sakti, A. D., Deliar, A., Soeksmantono, B., & Wikantika, K. (2022). Development of spatial model for food security prediction using remote sensing data in west java, Indonesia. *ISPRS International Journal of Geo-Information,* 11(5). https://doi.org/10.3390/ijgi11050284

Wang, C., Zhang, H., Wu, X., Yang, W., Shen, Y., Lu, B., & Wang, J. (2022). AUTS: A novel approach to mapping winter winter wheat by automatically updating training samples based on NDVI time series. *Agriculture (Switzerland),* 12(6). https://doi.org/10.3390/agriculture12060817

Xi, Y., Thinh, N. X., & Li, C. (2019). Preliminary comparative assessment of various spectral indices for built-up land derived from Landsat-8 OLI and Sentinel-2A MSI imageries. *European Journal of Remote Sensing,* 52(1), 240–252. https://doi.org/10.1080/22797254.2019.1584737

Xiao, G., Zhang, X., Niu, Q., Li, X., Li, X., Zhong, L., & Huang, J. (2024). Winter wheat yield estimation at the field scale using Sentinel-2 data and deep learning. *Computers and Electronics in Agriculture*, 216. https://doi.org/10.1016/j.compag.2023.108555

Yucebas, S., Dogan, M., & Genc, L. (2022). A C4.5 – Cart decision tree model for real estate price prediction and the analysis of the underlying features. *Konya Journal of Engineering Sciences,* 10(1), 147–161. https://doi.org/10.36306/konjes.1013833

Zhen, Z., Yunsheng, L., Moses, O. A., Rui, L., Li, M., & Jun, L. (2020). Hyperspectral vegetation indexes to monitor winter wheat plant height under different sowing

conditions. *Spectroscopy Letters*, 53(3), 194–206. https://doi.org/10.1080/00387010.2020.1726401

Zhou, Y., Wu, W., Wang, H., Zhang, X., Yang, C., & Liu, H. (2022). Identification of soil texture classes under vegetation cover based on Sentinel-2 data with SVM and SHAP techniques. *IEEE Journal of Selected Topics in Applied Earth Observations and Remote Sensing*, 15, 3758–3770. https://doi.org/10.1109/JSTARS.2022.3164140

Qiao, K., Zhu, W., Xie, Z., Wu, S., & Li, S. (2024). New three red-edge vegetation index (VI3RE) for crop seasonal LAI prediction using Sentinel-2 data. *International Journal of Applied Earth Observation nd Geoinformation*, *130*. https://doi.org/10.1016/j.jag.2024.103894